Novel Vortex Generator and Mode Converter for Electron Beams

P. Schattschneider*
Institut für Festkörperphysik, Technische Universität Wien, A-1040 Wien, Austria and LMSSMat (CNRS UMR 8579), Ecole Centrale Paris, F-92295 Châtenay-Malabry, France

M. Stöger-Pollach
University Service Centre for Electron Microscopy, Technische Universität Wien, A-1040 Wien, Austria

J. Verbeeck
EMAT, University of Antwerp, Groenenborgerlaan 171, 2020 Antwerp, Belgium
(Received 11 May 2012; published 22 August 2012)

A mode converter for electron vortex beams is described. Numerical simulations, confirmed by experiment, show that the converter transforms a vortex beam with a topological charge $m = \pm 1$ into beams closely resembling Hermite-Gaussian HG_{10} and HG_{01} modes. The converter can be used as a mode discriminator or filter for electron vortex beams. Combining the converter with a phase plate turns a plane wave into modes with topological charge $m = \pm 1$. This combination serves as a generator of electron vortex beams of high brilliance.

DOI: 10.1103/PhysRevLett.109.084801 PACS numbers: 41.85.−p, 03.65.Vf

The creation of free electron vortices [1,2] opened a new path to the study of matter. The first practical application was a filter for magnetic transitions, thus facilitating experiments in energy loss magnetic chiral dichroism [3,4]. Electron vortices up to topological charge $m \sim 100$ can now be produced routinely with holographic masks [5], and they may also occur naturally in the wave function of electrons after interaction with a crystal [6]. Potential applications range from the study of chiral structures over manipulation of nanoparticles, clusters, and molecules [7] to spin filters [8] and quantum computing [9]. Their local phase structure is similar to that of an electron in extremely strong magnetic fields [10]—on the order of 1000 T for vortices of nm dimension—which can make them a model system for the study of phenomena at such fields. One of the unique features of electron vortices is that, owing to their rotational component of probability current, they carry a magnetic moment, even for beams without spin polarization. This, the possibility to focus free electron vortices on a scale of one angstrom [11], and their strong interaction with matter makes them attractive.

Many properties of free electron vortices can be described by methods applied in singular optics, based on the theory of Nye and Berry [12]. Optical vortices are now used or proposed in many different research areas such as contrast improvement in astronomy [13] and microscopy [14], manipulation of microscopic particles [15], control of Bose-Einstein condensates [16], gravitational-wave detection [17], and quantum cryptography [9]. For a review of optical vortices and their application see Refs. [18,19].

For the control of vorticity of electron beams in transmission electron microscopy, mode converters would be of great interest. Such devices change the topological charge of an incident vortex by adding or subtracting charge units. An evident application is mode discrimination: Since vortex modes with charge m and $-m$ have the same spatial intensity distribution, a mode converter adding μ topological charges would yield modes with charge $\mu + m$ or $\mu - m$, which can be distinguished by their different radial profiles [8,20]. Moreover, a mode converter could increase the vorticity of an electron and thus the magnetic moment or simply be used to create a vortex from an incident plane wave (which has topological charge $m = 0$) by adding one unit of charge. The latter aspect is probably the most important one because the whole current would go into one vortex, contrary to the present holographic technique that blocks half of the intensity in the amplitude mask and distributes the remaining intensity into three fundamental modes and several higher harmonics. It goes without saying that such a device could exploit the entire brilliance of the electron source, resulting in an intensity gain of about an order of magnitude.

In laser optics, mode converters are used to change the topological charge of a beam. The idea is based on the linearity between Laguerre-Gaussian (LG) modes (which possess topological charge) on one hand and Hermite-Gaussian (HG) modes (which do not) on the other hand, combined with the phase shifting action of cylinder lenses. A particular setting of the lens parameters in combination with two cylinder lenses converts HG modes into LG modes [21].

Since an equivalent setup in the transmission electron microscopy is difficult to realize, we propose here a simple scheme for an electron mode converter, transforming electron beams with topological charge $m = \pm 1$ into HG modes and vice versa. A modification adding a phase plate

can convert a plane wave into a mode with topological charge $m = \pm 1$ and thus create a vortex.

Under paraxial conditions with an incident wave ψ_1 at a distance z_1 from the front focal plane (FFP) of a lens, the wave function in the observation plane that is at a distance z_2 from the back focal plane (BFP) is given by [22]

$$\psi_2(\mathbf{x}) = e^{ikx^2 z_1/2f^2} \int_\Pi \psi_1(\mathbf{q}) e^{i\chi(\mathbf{q})} e^{iq^2 z_2/2k} e^{-i\mathbf{q}\mathbf{x}} d^2q, \quad (1)$$

where k is the wave number and f is the focal length, with the phase

$$\chi(\mathbf{q}) = df(q_x^2 - q_y^2)/2k + C_s q^4/4k^3,$$

and the integral is over the aperture function Π. In order to distinguish the front focal and back focal planes, we use the variable $\mathbf{q}$ in the FFP and the variable $\mathbf{x}$ in the BFP. The parameter df is the astigmatic defocus (the stigmatic axes are in x and y directions), and C_s is the spherical aberration coefficient of the lens.

When both wave functions are in their respective focal planes, Eq. (1) collapses to the well-known Fourier transform between object and diffraction

$$\psi_2 = \mathrm{FT}[\psi_1 e^{i\chi}]. \quad (2)$$

Calculations are based on Eq. (1) and—where it applies—on Eq. (2).

In the following we adapt the approach of Beijersbergen *et al.* [21,23] for optical vortices that in the paraxial regime obey Eqs. (1) and (2) [24]. Any LG mode can be written as a linear superposition of HG beams. In the present context, we are interested in modes with topological charge $|m| = 1$. In the notation of Beijersbergen [21],

$$\mathrm{LG}_{10} = \frac{1}{\sqrt{2}}(\mathrm{HG}_{10} - i\mathrm{HG}_{01}), \quad (3)$$

$$\mathrm{LG}_{01} = \frac{1}{\sqrt{2}}(\mathrm{HG}_{10} + i\mathrm{HG}_{01}). \quad (4)$$

LG_{nm} beams carry topological charge $n - m$.

The basic mode converter imposes a relative phase shift of $\pi/2$ between the two components on the right hand side of Eq. (3). That transforms the wave into

$$\frac{1}{\sqrt{2}}(\mathrm{HG}_{10} - i^2\mathrm{HG}_{01}) = \frac{1}{\sqrt{2}}(\mathrm{HG}_{10} + \mathrm{HG}_{01}). \quad (5)$$

Noting that

$$\mathrm{HG}_{01}(\xi, \eta, z) = \frac{1}{\sqrt{2}}[\mathrm{HG}_{10}(x, y, z) + \mathrm{HG}_{01}(x, y, z)], \quad (6)$$

where new rescaled axes ξ, η, rotated by 45 degrees with respect to x, y are used, $\xi = (x+y)/\sqrt{2}$, $\eta = (x-y)/\sqrt{2}$, the output of the converter, Eq. (5) is a HG_{01} mode with its axis along the 45 degree direction. The same phase shift applied to Eq. (4) results in an HG_{10} mode, again with its axis along the 45 degree direction. So, the action of the phase shifting converter can be expressed in short as

$$\mathrm{LG}_{10} \overset{\pi/2}{\rightarrow} \mathrm{HG}_{01} \qquad \mathrm{LG}_{01} \overset{\pi/2}{\rightarrow} \mathrm{HG}_{10}. \quad (7)$$

Applying this idea to electrons raises two questions: (1) Are the vortex beams that can now be produced with holographic masks or emerging from a specimen after spin-polarized transitions [25] a sufficiently precise approximation to the LG_{10} and LG_{01} modes such that Eq. (7) holds? (2) Can we impose a phase shift of $\pi/2$ between the components with sufficient accuracy? In view of this question, simulations were not based on Eq. (7) but on the Schrödinger equation for vortex electrons in a magnetic lens [Eqs. (1) and (2)].

The vortex beams emerging from the holographic masks are superpositions of Bessel beams. A comparison of their radial distribution with an LG_{10} mode in the BFP shows that they are indeed very similar when the correct beam waist is chosen. The required phase shift between modes (task 2 above) is achieved exploiting the Gouy phase [26] of astigmatic beams. For HG beams of order (nm) it is [21]

$$\phi = (n + 1/2)\arctan\left(\frac{z - z_x}{z_R}\right) + (m + 1/2)\arctan\left(\frac{z - z_y}{z_R}\right), \quad (8)$$

where z_x, z_y are the positions of the astigmatic line foci.

Putting the beam waists at $z_x = z_R$, $z_y = -z_R$ as in Fig. 1, the relative Gouy phase shift between the fundamental modes HG_{10} and HG_{01} is, according to Eq. (8)

$$\Delta\phi = \arctan\left(\frac{z - z_R}{z_R}\right) - \arctan\left(\frac{z + z_R}{z_R}\right), \quad (9)$$

which at $z = 0$ is $\pi/2$. In other words, placing the observation plane at $z = 0$ in a lens with astigmatism $df = z_R$

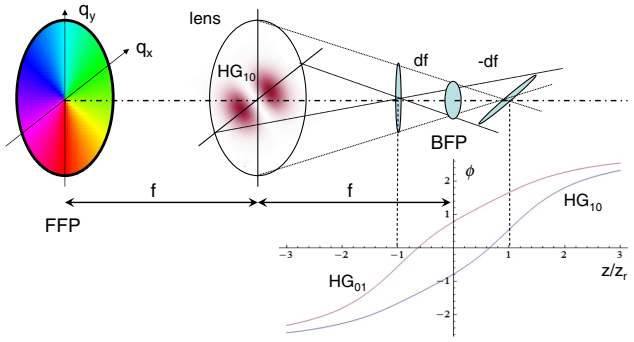

FIG. 1 (color online). Electron optical arrangement: A vortex fills the aperture in the FFP of a magnetic astigmatic lens. The phase is color coded (rainbow wheel). The astigmatic line foci along the x and y axes are at a mutual distance of $2df$. The vortex is composed of two phase-shifted HG-like components [Eq. (3)], one of which is symbolized as it passes the lens. Also drawn are the Gouy phases for the HG_{01} and the HG_{10} components for the case where the astigmatism equals the Rayleigh range, $df = z_R$. The observation plane is in the BFP midway between the line foci; there, the phase difference between the two HG modes is $\pi/2$.

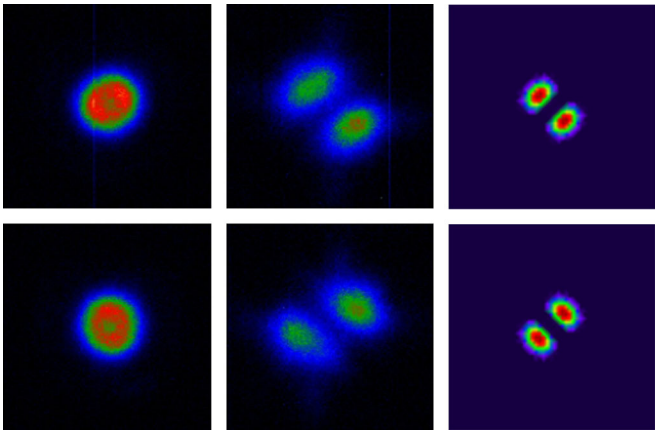

FIG. 2 (color online). Experimental mode conversion. Upper row: vortex with topological charge $m = -1$ after passage of a tunable lens. Left: astigmatism $df = 0$, yielding a focused vortex. Middle: astigmatism $df = 220$ nm. Right: simulation for 200 kV. Bottom row: same for $m = 1$. Squares have a side length of 5 nm. Intensities in all figures are in false color.

the phase shift between the two components is $\pi/2$. A complication is that the Gouy phase for non-Gaussian beams does not follow Eq. (9). Comparison of numerically obtained Gouy phases with that of a Gaussian beam of the same FWHM as the Airy disk results in an optimized astigmatism of $df = 220$ nm, almost identical to the Rayleigh range of the Gaussian beam. An astigmatic defocus of that value should induce the correct phase shift between the x and y components of the focused plane wave.

Figures 2 and 3 show experimental intensity distributions obtained on a TECNAI F20 microscope ($C_s = 1.2$ mm) at 200 kV with input vortices produced with a holographic fork mask in the FFP of the condenser lens, compared to numerical simulations. When the lens has no astigmatism, the well-known focused vortices are found in the BFP. The left column of Fig. 2 shows these beams. Tuning the astigmatism to $df = z_R$, the vortices with topological charge $m = \pm 1$ are converted into HG_{10}-like

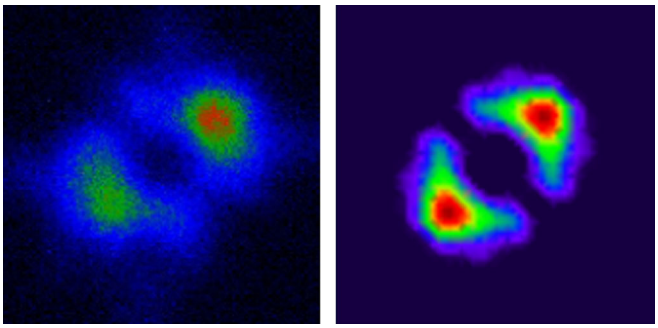

FIG. 3 (color online). Vortex with topological charge $m = 1$ after passage of a tunable lens with astigmatism $df = 700$ nm. Left: experiment. Right: simulation for 200 kV. Scale as in Fig. 2.

modes rotated by $\pm\pi/4$ about the optic axis, as shown in the center panels. The agreement with simulation (right panels) is excellent. Deviations (largely blurring) are caused by remaining lens aberrations, incomplete coherence, and the missing mode matching in this geometry [27]. We found that the structure of the converted modes is surprisingly stable under variations of astigmatism. Figure 3 shows the converted $m = 1$ mode for a larger astigmatism of $df = 700$ nm. The broken azimuthal symmetry in the HG modes seen in Fig. 2 can be used to analyze the topological charge on a sub-nm scale, with possible applications in crystallography [6], chirality [7], and spin-polarized electronic transitions [3,25].

Since such converters operate also in "reverse" mode, transforming HG into LG beams, one can use the device as a vortex generator without the need of an amplitude mask that blocks half the intensity. The entire signal would go into one vortex, rather than into three fundamental modes and higher harmonics. The difficulty lies in the experimental realization of HG electron beams. Contrary to laser optics where Gaussian beam profiles occur quite naturally, in electron optics there are plane or convergent waves limited by round apertures. But since the salient feature of the HG_{nm} modes is the phase shift of π between lobes, one can hope for a reasonable result using a phase plate. Such devices, proposed in 1942 to increase contrast by inducing a phase shift of $\pi/2$ [28], have seen a revival in the study of biological specimens [29]. Here, we use a Hilbert plate [29,30] (which induces a phase shift of π between the two lobes of a beam) not for contrast improvement but for phase inversion. Ideally that beam should resemble a $\pi/4$ rotated HG_{10} beam in the BFP. Figure 4(c) is an experimental image obtained at 86 kV from an incident convergent

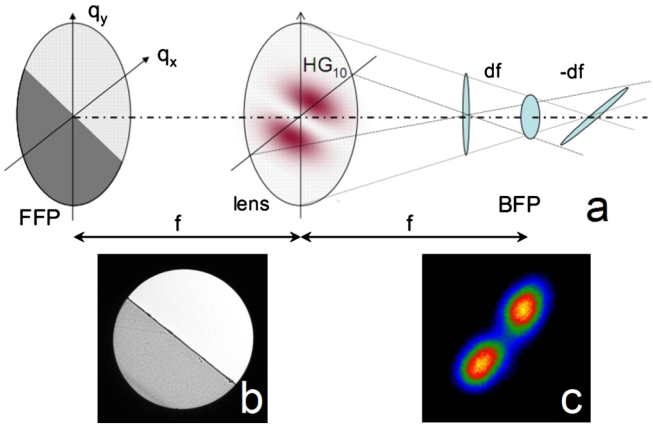

FIG. 4 (color online). Geometry for a vortex generator. (a) A Hilbert plate in the FFP imposes a phase shift of π on one half of the incident plane wave. This makes a rotated HG_{10}-like beam, here symbolized as it passes the lens. The Gouy phase shift of the astigmatic lens creates an LG_{10}-line beam in the BFP. (b) Shadow image of the phase plate. (c) Experimental p-orbital-like intensity in the BFP obtained with the phase plate and no astigmatism.

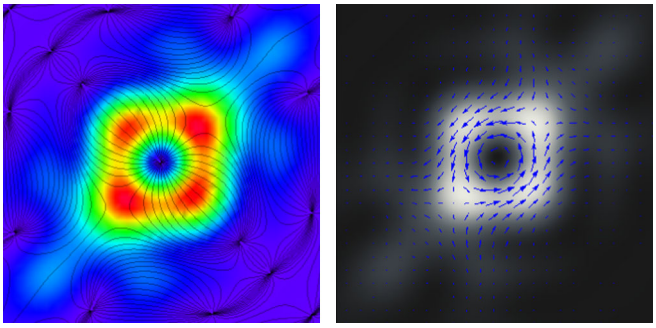

FIG. 5 (color online). Ideal output of the vortex generator. Left: intensity and cophasal lines increasing from 0 to 2π with the phase singularity in the center, characteristic of a topological charge $m = 1$. Right: same with superimposed circular quantum mechanical current density. Scale as in Fig. 2.

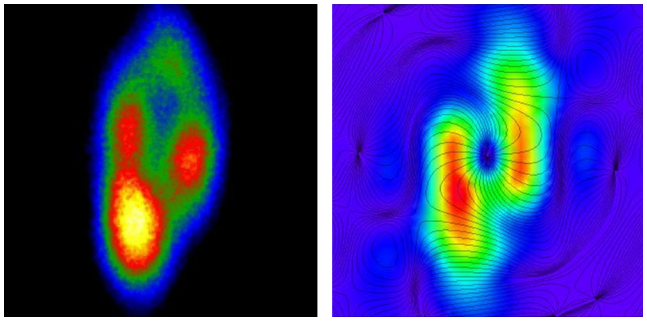

FIG. 6 (color online). Left: experimental vortex generator with nominal df as in Fig. 5. Right: optimized simulation (20% absorption, $df = 500$ nm, defocus 400 nm). Despite astigmatic distortions, the central phase singularity is well visible. Scale as in Fig. 2.

wave. The two lobes of the focused beam that resemble a p_x orbital are clearly discernible. The signal strength shows that ~90% of the intensity passing the aperture in the FFP goes into this mode. The corresponding wave functions reveal a phase difference of π. According to Eq. (6), the wave function is proportional to a superposition $HG_{10} + HG_{01}$. Figure 4(b) is an electron microscopical shadow image of the phase plate, cut from a commercially available Si-nitride thin film, projected on the probe forming aperture in the FFP.

When the vortex generator is activated, the Gouy phase shift of the astigmatic lens converts this HG mode into an LG_{10} beam in the BFP. Simulations based on Eq. (1) for an ideal phase plate are shown in Fig. 5. The phase singularity in the center of the left panel where all cophasal lines merge proves the presence of topological charge ($m = 1$ in the figure). The missing mode matching possibility in this geometry and the deviation from the Gaussian profiles cause the slight anisotropy of the charge density. However, the quantum mechanical current density $j = \rho\nabla\varphi$ (right panel) demonstrates clearly the vortex character of the output beam, containing ~90% of the incident intensity.

Results of a proof-of-principle experiment are shown in Fig. 6 (left) for an incident convergent wave and a nominal astigmatism corresponding to Fig. 5. Despite a linear distortion, four local maxima corresponding to the fourfold symmetry predicted in Fig. 5 can be seen. After variation of the simulation parameters (Fig. 6, right), it turned out that the main reasons for the disagreement are the strong absorption in the phase plate and a remaining defocus that is probably caused by cross talk of the magnetic field of the objective lens with that of the condenser. The experiment proves that the entire intensity of an incident convergent wave can be converted into a vortex. Optimizing the vortex generator will be challenging. A homogeneous phase plate of the necessary size, stability, and phase shift is difficult to produce and to maintain (beam damage and contamination will deteriorate the thin transparent film rapidly) but is not out of reach. An electrostatic Boersch-Hilbert plate would minimize absorption; use of a Kapitza-Dirac phase shifter [31] would also eliminate the contamination problem. Lack of mode matching, the difficulty of aligning the astigmatic axes with the edge of the phase plate, and the unavoidable cross talk of the objective lens field into the condenser limit the performance. A combination of two astigmatic lenses will probably improve the quality of the vortex generator.

In summary, we have demonstrated mode conversion for vortex electrons. The method can be used for discrimination of topological charge or for mode filtering. A variant including a phase plate can potentially generate vortex beams from incident plane electron waves with intensities surpassing that of the established fork mask technique by an order of magnitude.

P. S. acknowledges the financial support of the Austrian Science Fund, Project I543-N20. J. V. acknowledges support from the European Research Council under the 7th Framework Program (FP7), ERC Grant No. 246791—COUNTATOMS, and ERC Starting Grant No. 278510—VORTEX.

*schattschneider@ifp.tuwien.ac.at

[1] M. Uchida and A. Tonomura, Nature (London) **464**, 737 (2010).
[2] J. Verbeeck, H. Tian, and P. Schattschneider, Nature (London) **467**, 301 (2010).
[3] S. Lloyd, M. Babiker, and J. Yuan, Phys. Rev. Lett. **108**, 074802 (2012).
[4] P. Schattschneider, S. Rubino, C. Hbert, J. Rusz, J. Kunes, P. Novk, E. Carlino, M. Fabrizioli, G. Panaccione, and G. Rossi, Nature (London) **441**, 486 (2006).
[5] B. McMorran, A. Agrawal, I. Anderson, A. Herzing, H. Lezec, J. McClelland, and J. Unguris, Science **331**, 192 (2011).
[6] L. J. Allen, H. M. L. Faulkner, M. P. Oxley, and D. Paganin, Ultramicroscopy **88**, 85 (2001).
[7] H. Xin and D. Muller, Nature Nanotech. **5**, 764 (2010).

[8] E. Karimi, L. Marrucci, V. Grillo, and E. Santamato, Phys. Rev. Lett. **108**, 044801 (2012).
[9] S. Gröblacher, T. Jennewein, A. Vaziri, G. Weihs, and A. Zeilinger, New J. Phys. **8**, 75 (2006).
[10] M. Aidelsburger, M. Atala, S. Nascimbène, S. Trotzky, Y. A. Chen, and I. Bloch, Phys. Rev. Lett. **107**, 255301 (2011).
[11] J. Verbeeck, P. Schattschneider, S. Lazar, M. Stöger-Pollach, S. Löffler, A. Steiger-Thirsfeld, and G. van Tendeloo, Appl. Phys. Lett. **99**, 203109 (2011).
[12] J. Nye and M. Berry, Proc. R. Soc. A **336**, 165 (1974).
[13] G. Foo, D. M. Palacios, and G. A. Swartzlander, Jr., Opt. Lett. **30**, 3308 (2005).
[14] S. Fürhapter, A. Jesacher, S. Bernet, and M. Ritsch-Marte, Opt. Express **13**, 689 (2005).
[15] M. E. J. Friese, H. Rubinsztein-Dunlop, J. Gold, P. Hagberg, and D. Hanstorp, Appl. Phys. Lett. **78**, 547 (2001).
[16] M. F. Andersen, C. Ryu, P. Clade, V. Natarajan, A. Vaziri, K. Helmerson, and W. D. Phillips, Phys. Rev. Lett. **97**, 170406 (2006).
[17] M. Granata, C. Buy, R. Ward, and M. Barsuglia, Phys. Rev. Lett. **105**, 231102 (2010).
[18] G. Molina-Terriza, J. P. Torres, and L. Torner, Nature Phys. **3**, 305 (2007).
[19] S. Franke-Arnold, L. Allen, and M. Padgett, Laser Photonics Rev. **2**, 299 (2008).
[20] P. Schattschneider, M. Stöger-Pollach, S. Löffler, A. Steiger-Thirsfeld, J. Hell, and J. Verbeeck, Ultramicroscopy **115**, 21 (2012).
[21] M. W. Beijersbergen, L. Allen, H. E. L. O. van der Veen, and J. P. Woerdman, Opt. Commun. **96**, 123 (1993).
[22] W. Glaser, *Grundlagen der Elektronenoptik* (Springer-Verlag, Wien, 1952).
[23] M. J. Padgett and L. Allen, J. Opt. B **4**, S17 (2002).
[24] M. Born and E. Wolf, *Principles of Optics* (Cambridge University Press, Cambridge, England, 1999).
[25] P. Schattschneider, B. Schaffer, I. Ennen, and J. Verbeeck, Phys. Rev. B **85**, 134422 (2012).
[26] L. Gouy, Compt. Rend. Hébdom. Séances Acad. Sci. Paris **110**, 1251 (1890).
[27] In the observation plane the radii of curvature of the constituent waves have different signs. Mode matching uses two cylinder lenses to avoid this problem.
[28] F. Zernike, Physica (Amsterdam) **9**, 974 (1942).
[29] K. Nagayama, Eur. Biophys. J. **37**, 345 (2008).
[30] R. Danev, H. Okawara, N. Usuda, K. Kametani, and K. Nagayama, J. Biol. Phys. **28**, 627 (2002).
[31] H. Müller, J. Jin, R. Danev, J. Spence, H. Padmore, and R. M. Glaeser, New J. Phys. **12**, 073011 (2010).